



## Original Articles

# NLRP3 inflammasomes in macrophages drive colorectal cancer metastasis to the liver



Qiaoting Deng<sup>a,g,1</sup>, Yan Geng<sup>b,1</sup>, Liying Zhao<sup>c,1</sup>, Ru Li<sup>a</sup>, Zhigao Zhang<sup>a</sup>, Kun Li<sup>a</sup>, Rongliang Liang<sup>d</sup>, Xiangyang Shao<sup>a</sup>, Maoliang Huang<sup>e</sup>, Daming Zuo<sup>f</sup>, Yingsong Wu<sup>a,\*</sup>, Qiang Ma<sup>a,\*\*</sup>

<sup>a</sup> Institute of Antibody Engineering, School of Laboratory Medicine and Biotechnology, Southern Medical University, Guangzhou 510515, Guangdong, PR China

<sup>b</sup> Department of Gastroenterology, 303 Hospital of People's Liberation Army, Nanning 530021, PR China

<sup>c</sup> Department of General Surgery, Nanfang Hospital, Southern Medical University, Guangzhou, 510515, PR China

<sup>d</sup> Department of Laboratory Science, The Second Affiliated Hospital of Guangzhou University of Chinese Medicine, Guangzhou, Guangdong province, 510120, China

<sup>e</sup> Fuzhou Dingxiang Clinic, Fuzhou, Fujian 350028 China

<sup>f</sup> Institute of Molecular Immunology, School of Laboratory Medicine and Biotechnology, Southern Medical University, Guangzhou 510515, Guangdong, PR China

<sup>g</sup> Clinical Core Laboratory, Center for Precision Medicine, Meizhou People's Hospital (Huangtang Hospital), Meizhou Hospital Affiliated to Sun Yat-sen University, Meizhou 514031, PR China

## ARTICLE INFO

## Keywords:

NLRP3 inflammasome  
Macrophage  
Tumor microenvironment  
Colorectal cancer  
Liver metastasis

## ABSTRACT

Inflammation and immunity are important determinants of cancer initiation, promotion, and progression to cancer equilibrium or suppression. The NOD-like receptor family pyrin domain containing 3 (NLRP3) is an oligomeric intracellular immune receptor, and the main component of inflammasome. As a widely distributed effector of innate immunity, NLRP3 inflammasome affects development of many cancer types, but its exact role in colorectal cancer (CRC) is controversial. We found that cells with the macrophage (MΦ) marker CD68 and strong NLRP3 expression densely surrounded CRC tissue. The NLRP3 inflammasome was activated in MΦs by MΦ–CRC cell crosstalk; it resulted in faster migration of CRC cells, whereas blocking NLRP3 signaling suppressed CRC cell migration *in vitro*, and metastatic ability *in vivo*. NLRP3 signaling activation in MΦs can contribute to CRC cell migration and invasion.

## 1. Introduction

By 2030, the global burden of colorectal cancer (CRC) is expected to be more than 2.2 million new cases and 1.1 million deaths annually [1,2], with metastasis as the leading cause of these deaths [3]. Metastasis is a multistage process that requires cancer cells to escape from the primary tumor, survive in the circulation, seed at distant sites and grow. Each of these processes involves rate-limiting steps that are influenced by non-malignant cells of the tumor microenvironment [4,5].

Inflammation is considered as a hallmark of cancer [6]. Macrophages (MΦs), as primary components of the inflammation response system, are thought to modulate CRC metastasis to the liver [6,7]. Under stimulation by different factors, MΦs can be polarized to different types, with different biological activities, including removal of foreign pathogens in inflammatory reactions, or alternatively, orchestration of cytokine and chemokine networks in the tumor microenvironment that can contribute to tumor growth, angiogenesis,

migration, invasion, and metastasis [8,9]. Accordingly, abundant MΦ infiltration of tumor tissues is associated with poor prognosis in cancer patients [10], whereas systemic MΦ depletion inhibits primary tumor growth and metastasis *in vivo* [11]. However, the mechanisms of such results remain unclear.

The NOD-like receptor family pyrin domain containing 3 (NLRP3) is an oligomeric intracellular immune receptor, and the main component of inflammasome. The assembly of NLRP3 inflammasome can cleave dormant procaspase-1 into active caspase-1, which promotes maturation and secretion of IL-1β and IL-18, which drive inflammatory response [12,13]. Excessive secretion of IL-1β, mainly from MΦs [6], has been associated with cancer progression. Down-regulating IL-1β expression has been shown to suppress breast cancer invasiveness by inhibiting NF-κB [14]. IL-1β also has been found to promote metastasis by inducing epithelial–mesenchymal transition (EMT) or increasing matrix metalloproteinases (MMPs) activity in gastric adenocarcinoma (ADC) and bladder cancer [15,16]. Mature IL-1β can be released by human

\* Corresponding author.

\*\* Corresponding author.

E-mail addresses: [wg@smu.edu.cn](mailto:wg@smu.edu.cn) (Y. Wu), [mq@smu.edu.cn](mailto:mq@smu.edu.cn) (Q. Ma).

<sup>1</sup> These authors contributed equally to this work.

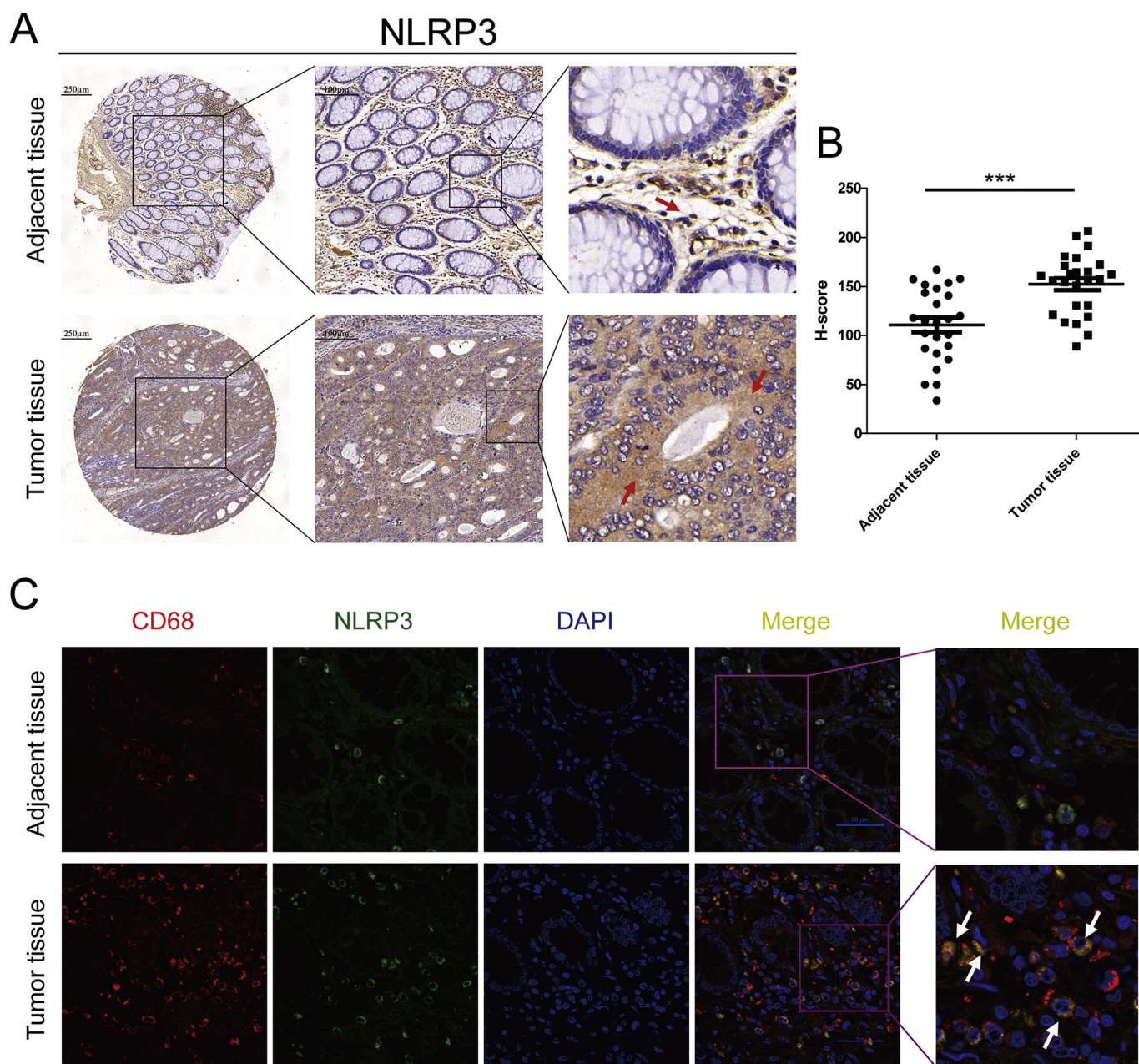


**Fig. 1. CD68<sup>+</sup> NLRP3-overexpressing macrophages (MΦs) along tumor boundary.** (A) Representative IHC images of NLRP3 expression in tumor–adjacent tissue pairs. (B) Histochemistry scores (H-scores: [% weakly stained cells × 1] + [% moderately stained × 2] + [% strongly stained × 3]) of NLRP3 expression in 25 tumor–adjacent tissue pairs. (C) Representative IF images of CD68 and NLRP3 expression in tumor–adjacent tissue pairs. \**P* < 0.05, \*\**P* < 0.01, \*\*\**P* < 0.001.

MΦs [12], whose NLRP3 inflammasomes are activated through pattern recognition receptors, including TLR2 and TLR4.

NLRP3 expression has been reported to be significantly upregulated in ADC and small-cell lung cancer, but absent or weak in non-small-cell lung cancer [17]. In hepatocellular carcinoma tissues, NLRP3 inflammasome components were significantly downregulated or even absent [18], whereas gastric cancer showed the opposite findings. Up-regulation of NLRP3 inflammasomes and their activation promotes migration and invasion of gastric cancer cells [19], which suggests that NLRP3 can promote malignancy. Thus, activated NLRP3 inflammasomes have contrasting roles in different tumor types.

The present study found that MΦs with high NLRP3 expression can surround CRC nests. MΦs were shown *in vitro* to migrate toward tumor cells, engage in crosstalk with CRC cells that activate NLRP3 inflammasomes and lead to IL-1β secretion, which then contributes to

CRC migration and metastasis. Conversely, CRC migration and metastasis were suppressed *in vitro* and *in vivo* by blocking NLRP3 signaling. These findings show that crosstalk between MΦs and CRC via NLRP3 signaling critically affects CRC migration and metastasis process. Our results might provide an alternative mechanism for the process of CRC metastasis.

## 2. Material and methods

### 2.1. Cell culture and differentiation

The cells used in this research were purchased from Chinese Academy of Sciences Cell Bank (Shanghai, CN). The human colon cancer cell line SW480, human monocyte cell line THP-1 and mouse colon cancer cell line MC38 were grown in RPMI 1640 (GibCo, New

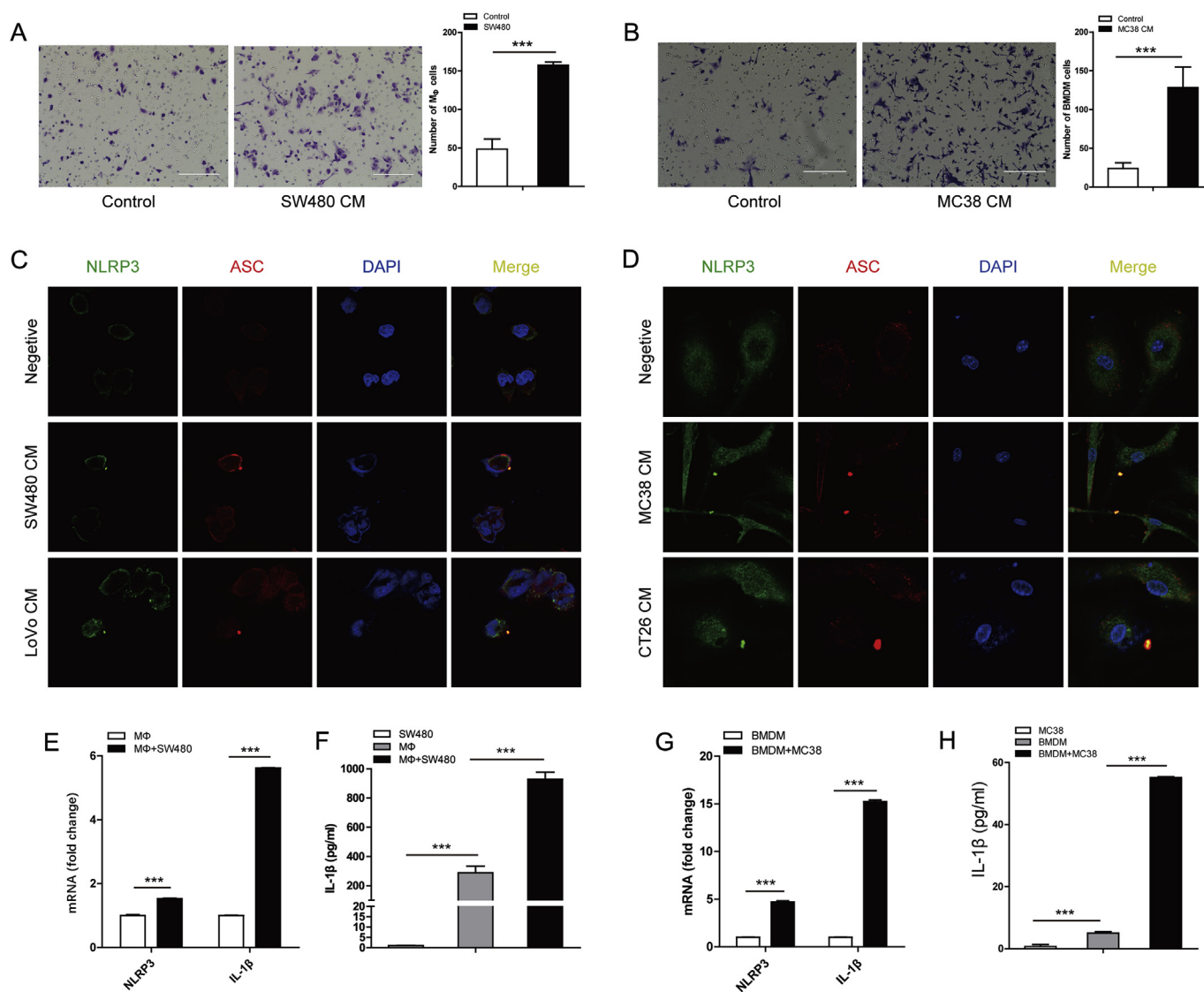


**Fig. 2.** NLRP3 inflammasomes in macrophages (MΦs) are activated by MΦ–colorectal cancer (CRC) crosstalk. (A, B) Chemotactic effect of CRC on MΦs; cell migration histogram. (C, D) NLRP3 inflammasome activation (NLRP3 co-stained with ASC) in MΦs. (E, G) *NLRP3* and *IL-1β* mRNA expression levels on MΦs after exposure to CRC conditioned medium (CM). (F, H) *IL-1β* secretion by MΦs after exposure to CRC CM. Data: mean  $\pm$  SE of 3 separate experiments. \* $P < 0.05$ , \*\* $P < 0.01$ , \*\*\* $P < 0.001$ .

York, US) with 10% fetal bovine serum (FBS; Biological Industries, Kibbutz, Israel), 100 U/ml penicillin and 100  $\mu$ g/ml streptomycin. The human colon cancer cell line LoVo and mouse colon cancer cell line CT26 were grown in DMEM (GibCo) with 10% FBS, 100 U/ml penicillin and 100  $\mu$ g/ml streptomycin. THP-1 cells were differentiated into MΦs by exposure to 200 nM phorbol-12-myristate-13-acetate (PMA; Sigma-Aldrich, St. Louis, MO) for 48 h. Mouse bone marrow monocytes (BMMs) were differentiated into bone marrow-derived MΦs (BMDMs) by exposure to 20 ng/ml granulocyte-macrophage colony-stimulating factor (GM-CSF, Peprotech, Southern California, US) for 7 days; the medium was changed every 3 days. BMDMs were grown in DMEM with 20% FBS, 100 U/ml penicillin and 100  $\mu$ g/ml streptomycin. Conditioned medium (CM) was collected as shown in supplementary materials (Supplementary Fig.S1). The CM was centrifuged at 3000 rpm/min for 5 min to clear any cell contaminants.

## 2.2. Bone marrow isolation

Mice were euthanized via cervical dislocation and disinfected with 75% alcohol. Their skin and tissue from legs were then removed with

scissors and the leg bones were dissected out and harvested. The top of each bone was removed with a scissors. We used syringes filled with 1 ml Hank's balanced salt solution (HBSS; GibCo) to flush bone marrow from leg bones. BMM isolates were harvested and cultured.

## 2.3. Quantitative real-time PCR

Total RNA was extracted from the cells using TRIzol reagent (Thermo Fisher, New York, US) according to the manufacturer's protocol. We synthesized cDNA from 1.0  $\mu$ g of total RNA using PrimeScript™ RT Master Mix reagent kit (Takara, Osaka, JP) in a final volume of 20  $\mu$ L. Real-time PCR was performed using SYBR® Premix Ex Taq™ II (Takara) on a 7500 Real Time PCR System (Applied Biosystems, Thermo Fisher). *GAPDH* was used as the internal control to correct for variations in cDNA content among the samples. Primer sequences for detected genes are described in supplementary materials (Supplementary Table S1). The dissociation curve indicated no amplification of nonspecific products in any reaction. Data were normalized to *GAPDH* expression levels and are presented as averages from three repeated experiments. Relative gene expression levels were calculated

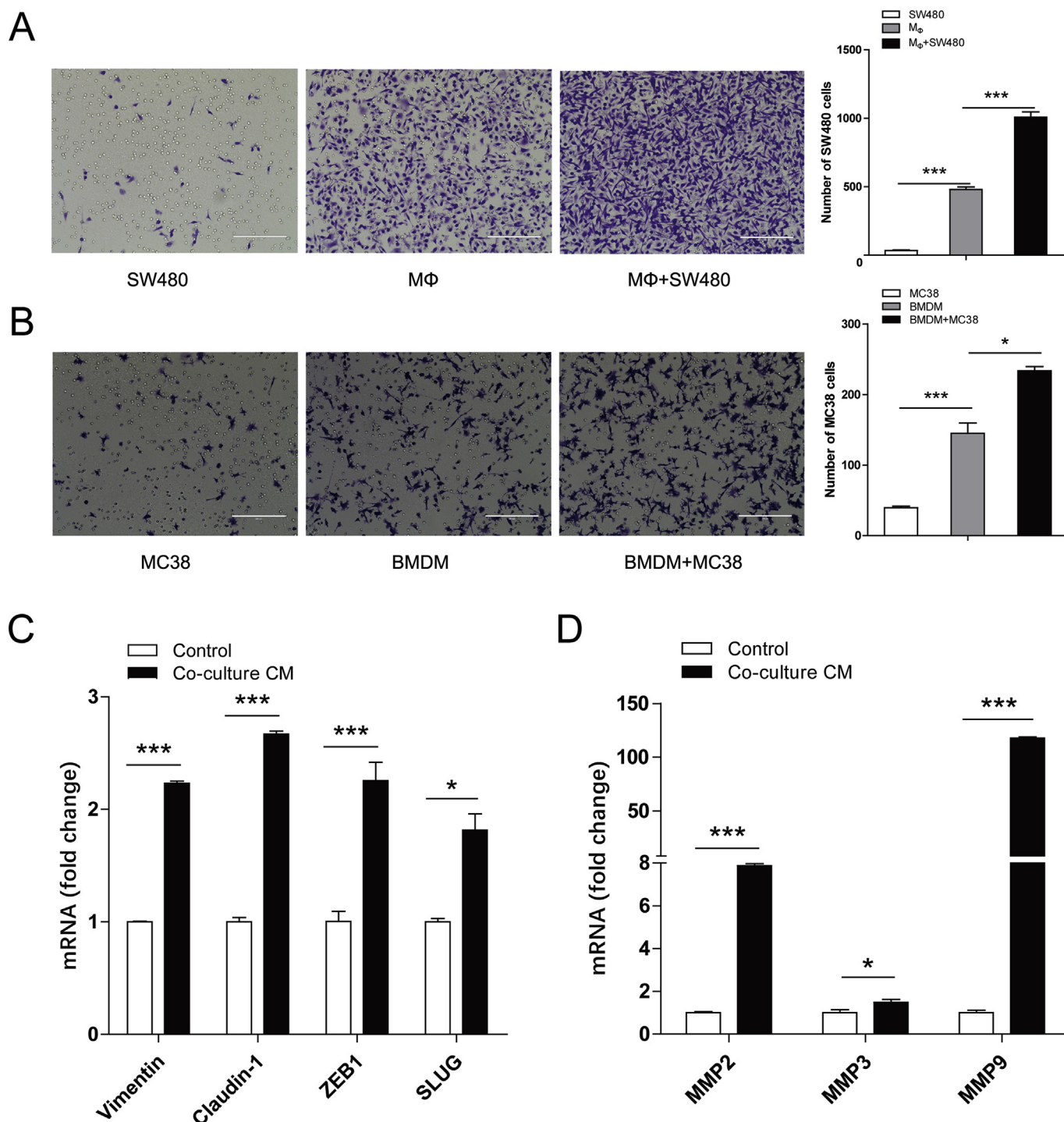


**Fig. 3. Crosstalk between macrophages and colorectal cancer (CRC) cells promotes CRC cell migration.** (A, B) Effect of co-culture conditioned medium (CM) on CRC migration with histogram. (C, D) mRNA expression of EMT markers and MMPs in SW480 cells after stimulation with co-culture CM. Data: mean ± SE of 3 separate experiments. \**P* < 0.05, \*\**P* < 0.01, \*\*\**P* < 0.001.

using the comparative Ct ( $\Delta\Delta C_t$ ) method; relative expression was calculated as  $2^{-\Delta\Delta C_t}$ , where *C<sub>t</sub>* represents the threshold cycle.

#### 2.4. Transwell assays

Migration assays were conducted using a 24-well Transwell chamber (Corning, New York, US) with 8- $\mu$ m pores. We added  $2 \times 10^5$  cells ( $1 \times 10^6$  cells/mL diluted by free medium) to the upper chamber, and 600  $\mu$ l of CM (chemoattractant) or RPMI 1640 (control) to the lower chamber. For blocking of IL-1 $\beta$ , anti-IL-1 $\beta$  neutralization

antibody (for SW480, 500 ng/ml, R&D systems; for MC38, 20  $\mu$ g/ml, R&D systems) or an isotype matched IgG control (R&D systems) was used. After incubation at 37 °C for appropriate time, the upper chambers were rinsed with PBS and fixed in 100% methanol for 10 min. The upper chambers were then rinsed with PBS again and stained with crystal violet for 10 min. Finally, cells inside the upper chambers were washed away, counted in five random fields at a magnification of  $\times 200$ , and then averaged.

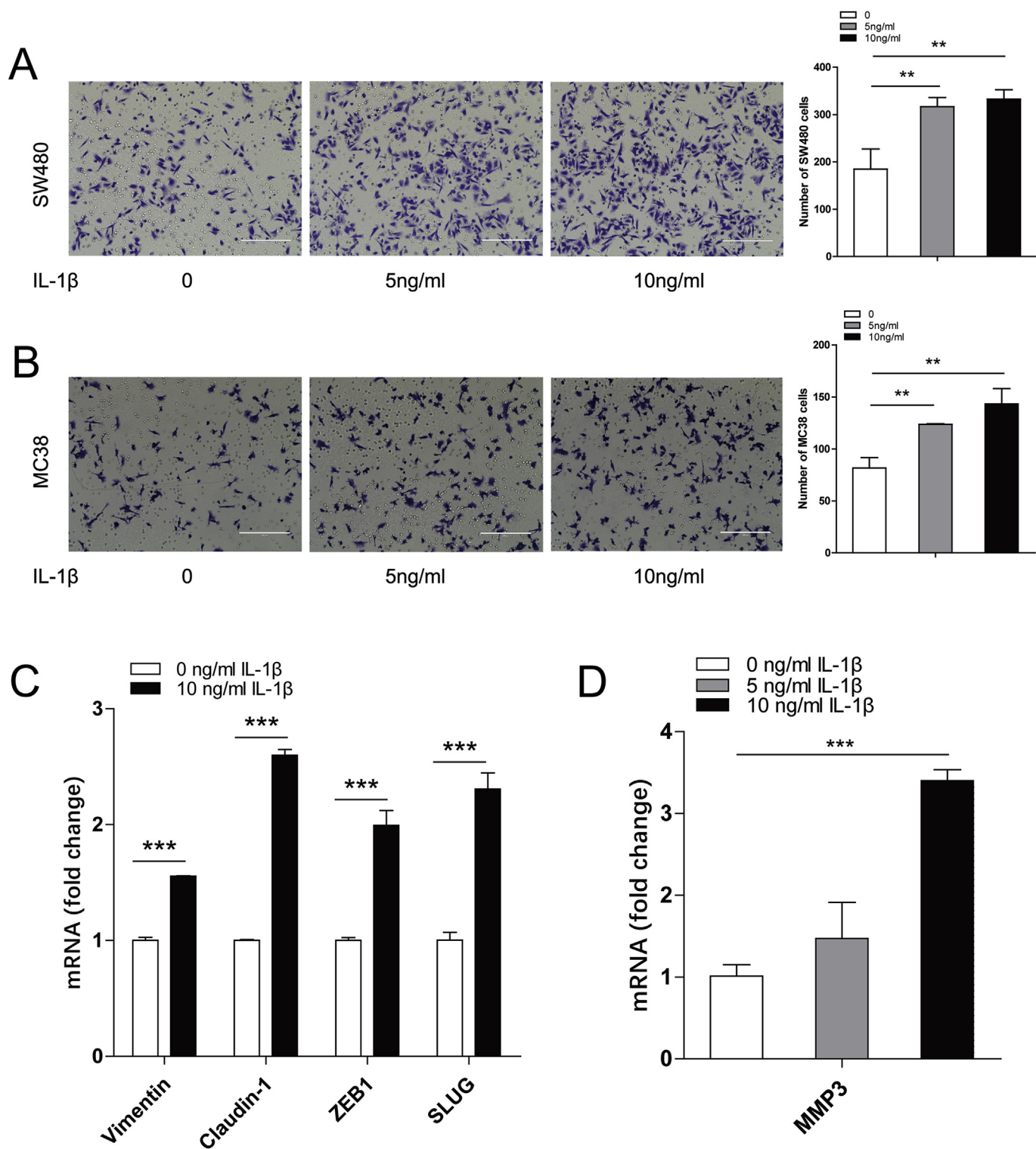


**Fig. 4. Induction of migration by rIL-1 $\beta$  in colorectal cancer (CRC) cells.** (A, B) Effect of IL-1 $\beta$  on CRC migration with histogram. (C, D) The mRNA expression of EMT markers and MMP3 on SW480 cells after exposure to IL-1 $\beta$ . Data: mean  $\pm$  SE of 3 separate experiments. \* $P$  < 0.05, \*\* $P$  < 0.01, \*\*\* $P$  < 0.001.

**2.5. Immunofluorescence confocal microscopy**

THP-1 cells were seeded on 15-mm glass-bottom cell culture dishes and differentiated into M $\Phi$ s by exposure to 200 nM PMA for 48 h, before stimulation with or without SW480/LoVo CM for 48 h. BMDM cells were seeded on 15-mm glass-bottom cell culture dishes for 12 h before stimulation with or without MC38/CT26 CM for 48 h. The cells were washed with PBS, fixed with 4% paraformaldehyde for 15 min, then

permeabilized with 0.25% TritonX-100 for 10 min and blocked with PBS containing 5% bovine serum albumin (BSA; Roche, Basel, SUI) for 1 h. Antibodies to NLRP3 (1:100; Abcam, London, UK) and apoptosis-associated speck like protein containing a caspase activation recruitment domain (ASC; 1:150; Abcam) were used for immunofluorescence (IF). The secondary antibodies, donkey anti-goat IgG-488 (1:300; Bioss, Beijing, CN) and goat anti-rabbit IgG-594 (1:500; Life, New York, US), were used for 1 h at room temperature. Thereafter, the samples were

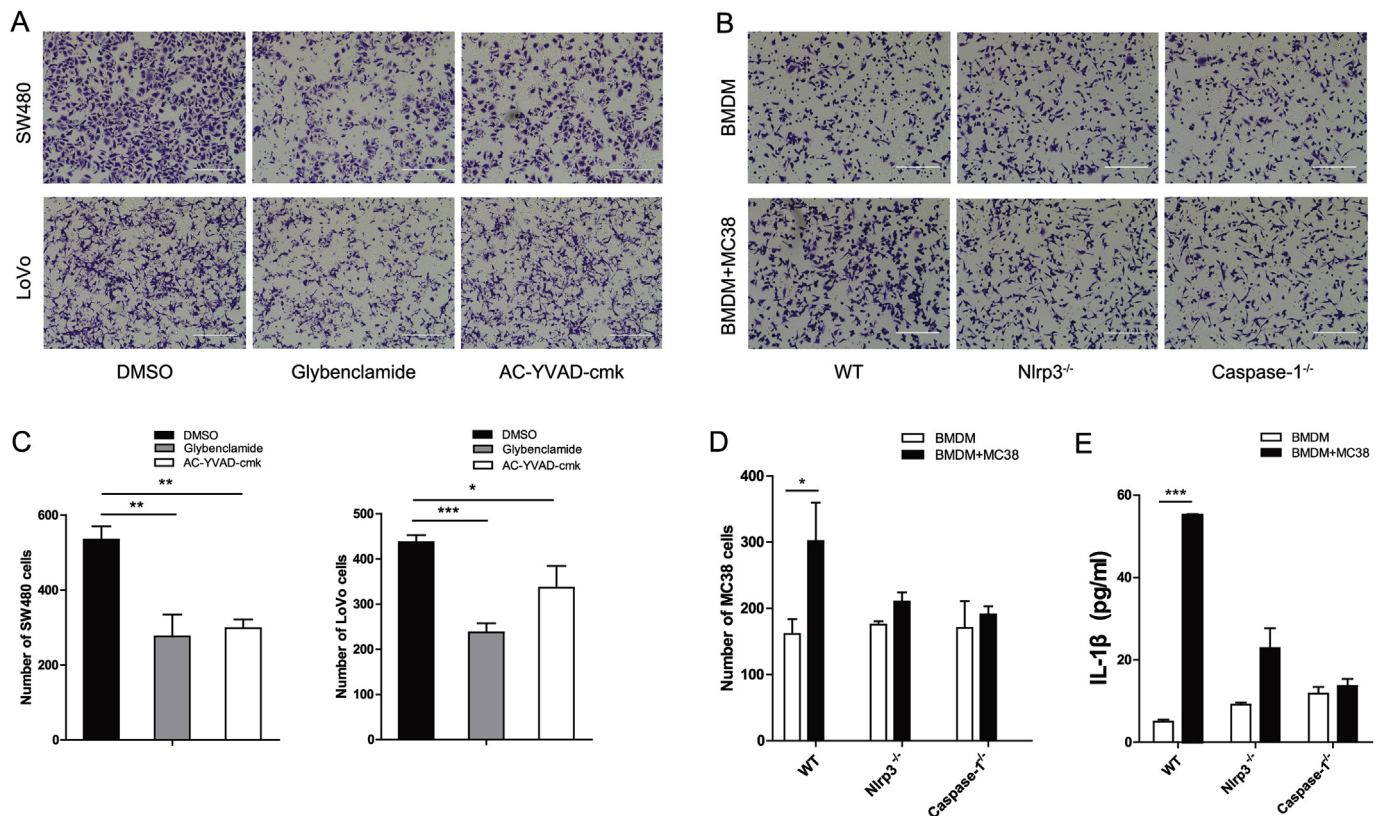


**Fig. 5. Blocking NLRP3 signaling with antagonists or gene knockout suppresses colorectal cancer (CRC) cell migration.** (A, C) Transwell assay shows inhibitors to suppress CRC migration towards macrophages, with histogram (C). (B, D) Effect of *NLRP3* or *caspase-1* knockout on the ability of BMDMs, with histogram of MC38 migration (D). (E) Secretion of IL-1 $\beta$  on BMDM after treatment with MC38 conditioned medium. Data: mean  $\pm$  SE of 3 separate experiments. \* $P < 0.05$ , \*\* $P < 0.01$ , \*\*\* $P < 0.001$ .

stained with DAPI (1:100, Beibokit, Beijing, CN) for 5 min. After being washed with PBS, confocal microscopic images (Nikon DS-FI1 microscope, magnification  $\times 600$ ) were taken and analyzed with NIS-Elements Basic Research software. Three independent experiments were performed.

## 2.6. IL-1 $\beta$ ELISA

THP-1 cells were differentiated into M $\Phi$ s by exposure to 200 nM PMA at a density of  $1 \times 10^6$  cells/well in 6-well plates and incubated for 48 h. The cells were then stimulated with SW480/LoVo CM for 24 h. RPMI 1640 was used as a control medium. The IL-1 $\beta$  concentration was measured in the culture medium with a human IL-1 $\beta$  ELISA kit (Abcam). BMDMs were seeded at a density of  $1.5 \times 10^5$  cells/well in 12-well plates and incubated for 12 h. The cells were then stimulated with MC38/CT26 CM for 48 h. RPMI 1640 was added as a control medium. The IL-1 $\beta$  concentration was measured in the culture medium with a mouse IL-1 $\beta$  ELISA kit (RayBiotech, Guangdong, CN). Three independent experiments were performed.

## 2.7. In vivo experiments

Animals care and experiments were approved by the Institutional Animal Care and Utilization Committee (IACUC). Homozygous *Nlrp3* knockout (*Nlrp3*<sup>-/-</sup>; B6.129S6-NLRP3<sup>tm1Bhk/J</sup>), and caspase-1 knockout (*Casp1*<sup>-/-</sup>; B6N.129S2-Casp1<sup>tm1Flv/J</sup>) mice were obtained from The Jackson Laboratories (Bar Harbor, ME). Wild-type (WT; C57BL/6) mice were purchased from Laboratory Animal Center of Southern Medical University (Guangdong, CN). All mice used in experiments were male, between 8 and 12 weeks of age, and they were kept under specific-pathogen-free conditions. To generate the model of

liver metastasis,  $5 \times 10^5$  MC38 cells in 100  $\mu$ l HBSS were injected into the spleen of each mouse ( $n = 6$  for each group). At 21 days after tumor cell inoculation, liver metastases were detected by micro-CT (IVIS Lumina II; PerkinElmer, Massachusetts, US). Then mice were euthanized, and their livers were collected and immediately stored in 4% paraformaldehyde, then embedded and sliced for immunohistochemical analysis or hematoxylin and eosin staining.

## 2.8. Immunohistochemistry

Paraformaldehyde-fixed, paraffin-embedded archival human colon cancer specimens or mice liver specimens were cut into 3-mm-thick sections and mounted onto glass slides, which were deparaffinized in xylol and rehydrated in an ethanol gradient. We then used 3% H<sub>2</sub>O<sub>2</sub> to inactivate the endogenous catalase; 0.01M sodium citrate solution was used to retrieve antigen. After blocking by 5% BSA, the slides were stained with anti-NLRP3 (1:100, Abcam). All stained tissues were visualized by incubation with goat anti-rabbit IgG (H + L)-HRP (1:100, Bioworld, Minnesota, US). After immunostaining with a DAB Kit (Genentech, California, US), all slides were manually counterstained with Mayer's hematoxylin. The stained tissues were scanned and analyzed with the EVOS<sup>®</sup> FL Auto (Life) at 100 $\times$  and 200 $\times$  magnifications.

## 2.9. H&E staining

Paraformaldehyde-fixed, paraffin-embedded archival human colon cancer specimens or mice liver specimens were cut into 3-mm-thick sections and mounted onto glass slides, which were deparaffinized in xylol and rehydrated in an ethanol gradient. The tissue slides were stained with hematoxylin and counterstained with eosin before being

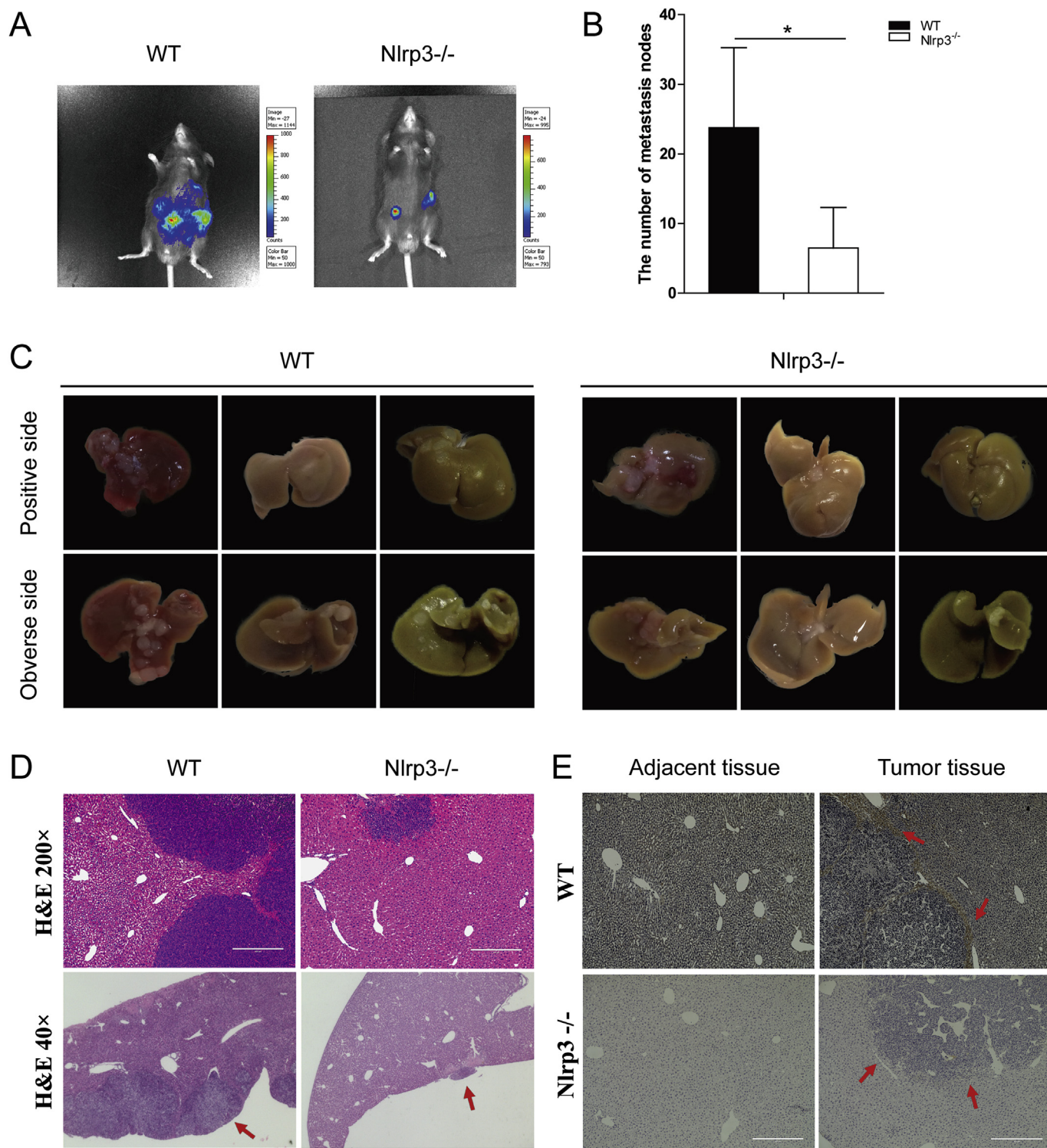


**Fig. 6.** *NLRP3* knockout impairs colorectal cancer (CRC) cells metastasis *in vivo*. (A) Day 21 after MC38 cell implantation in mice spleen, micro CT shows representative observable liver metastases in each group. (B) Number of visible metastasis nodes in livers. (C) Representative images of mice livers. (D) Representative HE images of cancer hepatic dissemination and metastasis (magnification, 40 × , 200 × ; red arrow, metastasis). (E) IHC analysis shows NLRP3 content in liver metastases from WT or NLRP3 <sup>-/-</sup> mice (magnification, 200 × ; red arrow, metastasis). \**P* < 0.05, \*\**P* < 0.01, \*\*\**P* < 0.001. (For interpretation of the references to color in this figure legend, the reader is referred to the Web version of this article.)

dehydrated in an ethanol gradient and mounted with coverslips. The stained tissues were scanned and analyzed with the EVOS<sup>®</sup> FL Auto (Life) at 100 × and 200 × magnifications.

### 2.10. Statistical analyses

SPSS software 20.0 was used for all real-time PCR analyses and statistical analysis of migration experiments. Prism software 5.0 (GraphPad Software, San Diego, CA, USA) was used for other statistical analyses and drawing bar charts. Adobe Illustrator CS6 was used for

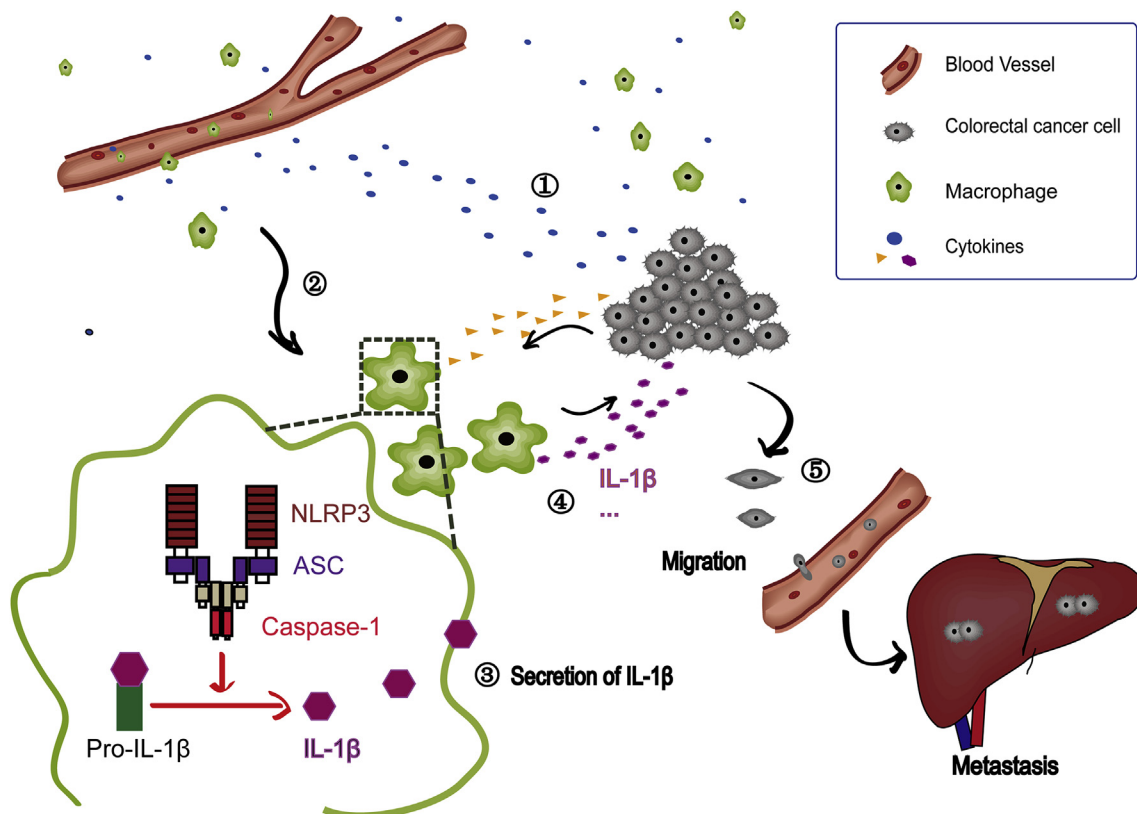


**Fig. 7. NLRP3 feedback in tumor microenvironment.** (1) Colorectal cancer (CRC) attracts macrophages (MΦs) by secreting cytokines. (2) After migrating to tumor stroma, MΦs are sensitized and polarized into a pro-tumoral phenotype. (3) CRC activates NLRP3 inflammasome and secretion of IL-1β by MΦs. (4) MΦs support CRC migration with IL-1β and other cytokines. (5) CRC occur EMT and up-regulate MMPs, thus promoting tumor progression and access to the vascular system, eventually causing metastasis.

editing the charts. All the data are presented as the mean  $\pm$  standard error of the mean (SEM).  $P < 0.05$  (Student's *t*-test) was considered significant. Three independent experiments were performed for each experiment.

### 3. Results

#### 3.1. NLRP3-overexpressing macrophages densely surrounded the tumor boundary

To explore the expression of NLRP3 in colorectal cancer tissues, we used IHC to detect NLRP3 expression in 25 sets of CRC tissues and adjacent normal tissues. We found that NLRP3 is overexpressed in tumor tissues, while significantly weaker IHC staining (independent sample *t*-test,  $t$  value =  $-4.283$ ,  $P < 0.001$ ) was seen in the adjacent normal colorectal tissues (Fig. 1A and B). The MΦ marker CD68 was shown by IF to be co-stained with NLRP3 in 6 samples of colon ADC (Fig. 1C). Compared with adjacent normal tissues, the tumor microenvironment contained more CD68<sup>+</sup> cells and higher NLRP3 expression. These results suggest that NLRP3 inflammasomes in MΦs in the tumor microenvironment may affect CRC developments.

#### 3.2. NLRP3 inflammasomes in MΦs are activated by MΦ–CRC cell crosstalk

To investigate whether communication between MΦ and CRC cells affected MΦs behavior, we exposed MΦs to CM derived from CRC. This resulted in a significant increase in MΦs migration. CM from SW480 cells caused a three-fold increase in MΦ migration (Fig. 2A), and CM from MC38 cells caused a five-fold increase in BMDM migration (Fig. 2B). Similar results appear in CT26 CM (Supplementary Fig. S2A).

We therefore hypothesized that MΦs migrate to tumors and are affected by the tumor microenvironment. After stimulation with SW480 CM for 48 h, MΦs showed up-regulation of NLRP3 and IL-1β (Fig. 2E). Up-regulated NLRP3 and IL-1β were also seen in BMDMs after treatment with CM from MC38 cells (Fig. 2G). Similar results appeared in LoVo or CT26 CM (Supplementary Fig. 2B). The enhanced presence of NLRP3 and ASC, and caspase-1 cleavage indicate intracellular activation of inflammasomes [20]. Confocal microscopy showed NLRP3 and ASC co-localization in MΦs after stimulation with SW480 or LoVo CM for 48 h (Fig. 2C). After stimulation with MC38 or CT26 CM for 48 h, NLRP3 also formed large speck-like structures and co-localized with ASC in BMDMs (Fig. 2D). Activation of NLRP3 inflammasomes culminated in caspase-1 activation and IL-1β secretion. The IL-1β concentration was measured in the CM. Compared with MΦ alone, CM from SW480–MΦ co-cultures caused 2-fold increase in IL-1β secretion (Fig. 2F). Similar results appear in LoVo–MΦ co-cultures (Supplementary Fig. S2C). In addition, MC38–BMDM co-cultures caused 10-fold increase in IL-1β secretion compared with BMDM alone (Fig. 2H). These observations suggest that interactions between MΦs and CRC activate NLRP3 inflammasomes and increase IL-1β secretion in MΦs.

#### 3.3. Communication between MΦ and CRC cells promotes CRC cell migration

To further confirm the role of communication between MΦs and CRC in the tumor microenvironment, we established an *in vitro* co-culture model. Human monocyte cell line THP-1 cells were differentiated into MΦs by exposure to 200 nM PMA for 48 h. BMDMs were generated from mouse bone marrow using GM-CSF to polarize BMDMs toward BMDMs. Exposing CRC cells to co-cultured CM resulted in significantly increased migration by SW480 and MC38 cells (Fig. 3A and

B). CM from SW480–M $\Phi$  co-cultures caused a significant increase in SW480 migration compared with M $\Phi$  CM alone (Fig. 3A). Similarly, MC38–BMDM CM also caused an increase in MC38 migration (Fig. 3B). Such effects could be abolished by the treatment of IL-1 $\beta$  neutralized antibody (Supplementary Fig. S3). Expression of EMT markers and MMPs on SW480 cells also were assessed by real time-PCR. After treatment with co-cultured CM, significantly increased expression of Vimentin, Claudin-1, ZEB1, Slug and MMP-2, MMP-3, MMP-9 was seen in SW480 cells (Fig. 3C and D). These observations suggest that interactions between M $\Phi$ s and CRC shift cancer cells to a more migratory phenotype.

### 3.4. Induction of migration by rIL-1 $\beta$ in colon cancer cells

In view of greater IL-1 $\beta$  secretion in co-cultured CM, we hypothesized that IL-1 $\beta$  might promote CRC migration directly. We exposed CRC to different concentrations of recombinant IL-1 $\beta$ , which resulted in significantly increased migration of SW480 or MC38 cells (Fig. 4A and B). LoVo cells showed similar results (Supplementary Fig. S4). Moreover, expressions of Vimentin, Claudin-1, ZEB1, Slug and MMP-3 in SW480 cells were up-regulated after exposure to IL-1 $\beta$  (Fig. 4C and D). These results imply that interactions between M $\Phi$  and CRC cells promote CRC cell migration, possibly mediated by IL-1 $\beta$ .

### 3.5. Blocking NLRP3 signaling with antagonists or gene knockout suppressed CRC cell migration

Because of the contribution of NLRP3 inflammasome to the pathology of various inflammation-driven diseases, we have attempted to develop NLRP3 and caspase-1 antagonists, which we expected to decrease CRC cell migration. Here, we evaluated the feasibility of targeting inflammasomes for human CRC therapy with a NLRP3 antagonist, glibenclamide (Sigma-Aldrich), and a caspase-1 antagonist, AC-YVAD-cmk (Sigma-Aldrich). These antagonists showed little cytotoxicity to SW480 and LoVo cancer cells or M $\Phi$  cells (Supplementary Fig. S5). We found these antagonists to inhibit NLRP3 inflammasome-induced chemotaxis of SW480 cells and LoVo cells (Fig. 5A and C). Bone marrow cells from *Nlrp3*- or *Casp1*-knockout and WT mice had been extracted and polarized to BMDMs by GM-CSF. After treatment with MC38 CM, *Nlrp3*<sup>-/-</sup> or *Casp1*<sup>-/-</sup> BMDMs showed less IL-1 $\beta$  secretion (Fig. 5E), and demonstrated reduced MC38 migration in the MC38–BMDM co-culture model (Fig. 5B, D) than did WT cells. Taken together, these results confirm that M $\Phi$ s can significantly promote migration of CRC by activating NLRP3 inflammasomes and increasing IL-1 $\beta$  secretion, which can be inhibited by blocking NLRP3 signaling.

### 3.6. NLRP3 knockout impair CRC cells metastasis in vivo

To evaluate the role of NLRP3 in tumor progression and metastasis *in vivo*, we used *Nlrp3* knockout mice and WT C57 mice to establish a metastasis model. We injected  $5 \times 10^5$  MC38 cells in 100  $\mu$ l HBSS into the spleen of each mouse to generate a model of liver metastasis. After 21 days, liver metastasis lesions were examined by micro-CT. The mice were then sacrificed, and their livers were examined. We observed that the *Nlrp3*<sup>-/-</sup> mice had fewer liver metastasis nodes than did the WT mice (Fig. 6A–C). Moreover, the *Nlrp3*<sup>-/-</sup> mice showed less hepatic dissemination and metastasis of cancer cells (Fig. 6D). In addition, we detected NLRP3 content in the liver metastases of the WT mice by IHC analysis, and found higher expression of NLRP3 along the tumor boundaries (Fig. 6E). These results suggest that NLRP3 inflammasomes promote tumor progression and *Nlrp3* knockout impairs CRC metastasis *in vivo*.

## 4. Discussion

Immune cells, including M $\Phi$ s and lymphocytes, together with

fibroblasts, neutrophils and vascular endothelial cells, infiltrate tumor tissues to form the tumor microenvironment [8]. The infiltration of large numbers of M $\Phi$ s into tumor cells is considered to be a hallmark of cancer severity and malignancy; thus these M $\Phi$ s have been called tumor-associated M $\Phi$ s (TAMs) [21]. TAMs can differentiate into pro-tumoral or M2 M $\Phi$ s; in high density, they are thought to increase vessel density, immunosuppression, and proliferation of cancer cells in malignant tumors [22]. In the present study, we found that M $\Phi$ s, which were identified as CD68<sup>+</sup> cells through IF, were densely located in tumor microenvironments of CRC tissue samples (Fig. 1C). Numbers of CD68<sup>+</sup> cells were significantly higher in the CRC microenvironment compared with normal tissues. These M $\Phi$ s were mostly observed around tumor nests, which implies that M $\Phi$ s migrate toward tumor tissues.

Compared with normal tissues, the CD68<sup>+</sup> cells localized in the tumor microenvironment showed higher NLRP3 expression and activation (Fig. 1C). NLRP3 inflammasome formation and caspase-1 activation increase in some human immune diseases processes [23]. However, the role of NLRP3 expression in tumor progression is controversial. Differential expression of NLRP3 inflammasomes had been reported in lung cancer cell lines and tissues [17]. Up-regulation and activation of NLRP3 inflammasomes promote migration and invasion of gastric cancer cells, whereas expression of NLRP3 inflammasome components are significantly down-regulated or even absent in hepatocellular carcinoma tissues [18,19].

The role of the NLRP3 inflammasome in the CRC progression has not been widely studied. To evaluate the role of NLRP3 inflammasomes in CRC progression, we cultured M $\Phi$ s with CM derived from CRC cells to establish a co-culture system, and found increased activation of NLRP3 inflammasomes and IL-1 $\beta$  secretion of in M $\Phi$ s, after treatment with CRC CM (Fig. 2). These results suggest that interactions between M $\Phi$ s and CRC cells may shift cancer cells to a more migratory phenotype (Fig. 3).

Interestingly, after stimulation with co-cultured CM, CRC cells were characterized by a spindle-like shape, with up-regulated expression of claudin-1, Zeb1 and vimentin (Fig. 3C). These morphological changes and upregulation of EMT markers, as cells lose their epithelial characteristics and acquire mesenchymal characteristics, such as loss of adherens junctions and increased migration ability, are associated with cancer progression and metastasis [24,25]. Abnormal EMT changes can promote cancer cell migration and systemic dissemination [26,27]. Additionally, interactions between M $\Phi$  and CRC cells also could enhance expression of MMP-2, MMP-3 and MMP-9, which are described as pro-tumorigenic MMPs, a superfamily of zinc-dependent endopeptidases that are known to facilitate tumor cell invasion and metastasis by degrading the extracellular matrix (Fig. 3D) [21,28,29]. These findings indicate that M $\Phi$ –CRC-cell crosstalk promote CRC migration and metastasis by inducing EMT and increasing MMP activity.

Furthermore, in consideration of increased IL-1 $\beta$  secretion after exposure to co-culture CM, we exposed CRC samples to different concentrations of recombinant IL-1 $\beta$ , which resulted in significantly increased migration, and upregulation of mesenchymal markers and MMP3 (Fig. 4). These results are consistent with previous work. Down-regulation of IL-1 $\beta$  inhibits invasiveness in breast cancer, whereas excessive secretion of IL-1 $\beta$  promotes tumor metastasis in gastric ADC and bladder cancer [14–16]. In fact, mature IL-1 $\beta$  can be released by human M $\Phi$ s through the activation of NLRP3 inflammasomes [6]. These findings demonstrated that activating NLRP3 inflammasomes in M $\Phi$ s drives cancer cell migration in the tumor microenvironment via the secretion of IL-1 $\beta$ .

To confirm the contribution of NLRP3 inflammasomes to cancer progression, M $\Phi$ s were treated with antagonists to NLRP3 (glibenclamide) or caspase-1 (AC-YVAD-cmk), to suppress their promotion of CRC migration. Similarly, after treatment with MC38 CM, BMDMs from *Nlrp3*<sup>-/-</sup> or *Casp1*<sup>-/-</sup> mice showed lower IL-1 $\beta$  secretion and MC38 migration compared with BMDMs from WT mice (Fig. 5).

Accordingly, *Nlrp3*<sup>-/-</sup> mice had decreased liver metastasis in mice models compared with WT mice (Fig. 6A and B). Moreover, the *Nlrp3*<sup>-/-</sup> mice had less hepatic dissemination of cancer cells (Fig. 6C). These findings indicate that MΦs migrate toward tumors and further drive the CRC cells migration via activation of NLRP3 inflammasomes.

In conclusion, the NLRP3 signaling activation during MΦ–CRC cell crosstalk drives CRC migration and metastasis. Our results are shown in a diagram (Fig. 7). Several molecular and cellular triggers for the activation of NLRP3 inflammasomes have been proposed, including K<sup>+</sup> efflux, reactive oxygen species, and mitochondrial dysfunction [12]. However, which molecules and pathways are triggers for MΦ inflammasome activation still need to be explored. How tumor cells activate the NLRP3 inflammasome in MΦs to transform their phenotypes will be our next step. Further research on communication between MΦs and tumors will clarify the mechanism by which NLRP3 drives CRC metastasis.

### Conflicts of interest

The authors declare no competing financial interests.

### Abbreviations

ADC, Adenocarcinoma; BMDM, Bone marrow-derived macrophage; BMM, Bone marrow monocytes; BSA, Bovine serum albumin; cDNA, Complementary DNA; CM, Conditioned medium; CRC, Colorectal cancer; EMT, Epithelial–mesenchymal transition; FBS, Fetal bovine serum; GM-CSF, Granulocyte macrophage-colony stimulating factor; HE, Hematoxylin and eosin stain; IF, immunofluorescence; M<sub>Φ</sub>, Macrophage; MMP, Matrix metalloprotein; PMA, Phorbol-12-myristate-13-acetate; TMA, Tumor-associated macrophage.

### Acknowledgements

The work was supported by the National Natural Science Foundation of China [81772133 and 81741133]; Guangdong Natural Science Fund of China [2016A030313529], and Outstanding Young Teachers Training Program of China [YQ2015037]; Guangxi Natural Science Fund 2017GXNSFDA198051 and 2016GXNSFAA380313. We thank the Department of Pathology, Nanfang Hospital for providing colorectal cancer tissue sections. We also thank the Department of Neurobiology, School of Basic Medicine, Southern Medical University for their help with confocal microscopy. We thank Marla Brunner, from Liwen Bianji, Edanz Group China ([www.liwenbianji.cn/ac](http://www.liwenbianji.cn/ac)), for editing the English text of a draft of this manuscript.

### Appendix A. Supplementary data

Supplementary data to this article can be found online at <https://doi.org/10.1016/j.canlet.2018.10.030>.

### References

- [1] M. Arnold, M.S. Sierra, M. Laversanne, I. Soerjomataram, A. Jemal, F. Bray, Global patterns and trends in colorectal cancer incidence and mortality, *Gut* 66 (2017) 683–691.
- [2] L.A. Torre, F. Bray, R.L. Siegel, J. Ferlay, J. Lortet-Tieulent, A. Jemal, Global cancer statistics, *CA A Cancer J. Clin.* 65 (2015) (2012) 87–108.
- [3] A.G. Clark, D.M. Vignjevic, Modes of cancer cell invasion and the role of the microenvironment, *Curr. Opin. Cell Biol.* 36 (2015) 13–22.
- [4] J.A. Joyce, J.W. Pollard, Microenvironmental regulation of metastasis, *Nat. Rev. Canc.* 9 (2009) 239–252.
- [5] S. Serres, E.R. O'Brien, N.R. Sibson, Imaging angiogenesis, inflammation, and metastasis in the tumor microenvironment with magnetic resonance imaging, *Adv. Exp. Med. Biol.* 772 (2014) 263–283.
- [6] A. Lasry, A. Zinger, Y. Ben-Neriah, Inflammatory networks underlying colorectal cancer, *Nat. Immunol.* 17 (2016) 230–240.
- [7] D. Hanahan, R.A. Weinberg, Hallmarks of cancer: the next generation, *Cell* 144 (2011) 646–674.
- [8] Y. Komohara, Y. Fujiwara, K. Ohnishi, M. Takeya, Tumor-associated macrophages: potential therapeutic targets for anti-cancer therapy, *Adv. Drug Deliv. Rev.* 99 (2016) 180–185.
- [9] R.A. Franklin, W. Liao, A. Sarkar, M.V. Kim, M.R. Bivona, K. Liu, E.G. Pamer, M.O. Li, The cellular and molecular origin of tumor-associated macrophages, *Science* 344 (2014) 921–925.
- [10] A. Mantovani, T. Schioppa, C. Porta, P. Allavena, A. Sica, Role of tumor-associated macrophages in tumor progression and invasion, *Cancer Metastasis Rev.* 25 (2006) 315–322.
- [11] Y. Zhang, W. Sime, M. Juhas, A. Sjölander, Crosstalk between colon cancer cells and macrophages via inflammatory mediators and CD47 promotes tumour cell migration, *Eur. J. Canc.* 49 (2013) 3320–3334.
- [12] Y. He, H. Hara, G. Núñez, Mechanism and regulation of NLRP3 inflammasome activation, *Trends Biochem. Sci.* 41 (2016) 1012–1021.
- [13] A. Stutz, D.T. Golenbock, E. Latz, Inflammasomes: too big to miss, *J. Clin. Invest.* 119 (2009) 3502–3511.
- [14] M. Jeon, J. Han, S.J. Nam, J.E. Lee, S. Kim, Elevated IL-1β expression induces invasiveness of triple negative breast cancer cells and is suppressed by zerbivone, *Chem. Biol. Interact.* 258 (2016) 126–133.
- [15] R. Matsumoto, M. Tsuda, K. Yoshida, M. Tanino, T. Kimura, H. Nishihara, T. Abe, N. Shinohara, K. Nonomura, S. Tanaka, Aldo-keto reductase 1C1 induced by interleukin-1β mediates the invasive potential and drug resistance of metastatic bladder cancer cells, *Sci. Rep.* 6 (2016).
- [16] Q. Huang, F. Lan, X. Wang, Y. Yu, X. Ouyang, F. Zheng, J. Han, Y. Lin, Y. Xie, F. Xie, W. Liu, X. Yang, H. Wang, L. Dong, L. Wang, J. Tan, IL-1β-induced activation of p38 promotes metastasis in gastric adenocarcinoma via upregulation of AP-1/c-fos, MMP2 and MMP9, *Mol. Canc.* 13 (2014) 18.
- [17] H. Kong, Y. Wang, X. Zeng, Z. Wang, H. Wang, W. Xie, Differential expression of inflammasomes in lung cancer cell lines and tissues, *Tumor Biol.* 36 (2015) 7501–7513.
- [18] Q. Wei, K. Mu, T. Li, Y. Zhang, Z. Yang, Deregulation of the NLRP3 Inflammasome in Hepatic Parenchymal Cells during Liver Cancer Progression, Laboratory Investigation, 2014.
- [19] Y. Xu, H. Li, W. Chen, X. Yao, Y. Xing, X. Wang, J. Zhong, G. Meng, Mycoplasma hyorhinis activates the NLRP3 inflammasome and promotes migration and invasion of gastric cancer cells, *PLoS One* 8 (2013) e77955.
- [20] Y. Geng, Q. Ma, Y.N. Liu, N. Peng, F.F. Yuan, X.G. Li, M. Li, Y.S. Wu, B.L. Li, W.B. Song, W. Zhu, W.W. Xu, J. Fan, L. Su, Heatstroke induces liver injury via IL-1β and HMGB1-induced pyroptosis, *J. Hepatol.* 63 (2015) 622–633.
- [21] K. Vinnakota, Y. Zhang, B.C. Selvanesan, G. Topi, T. Salim, J. Sand-Dejmek, G. Jonsson, A. Sjölander, M2-like macrophages induce colon cancer cell invasion via matrix metalloproteinases, *J. Cell. Physiol.* 232 (2017) 3468–3480.
- [22] Y. Komohara, M. Jinushi, M. Takeya, Clinical significance of macrophage heterogeneity in human malignant tumors, *Cancer Sci.* 105 (2014) 1–8.
- [23] M. Lamkanfi, V.M. Dixit, Inflammasomes and their roles in health and disease, *Annu. Rev. Cell Dev. Biol.* 28 (2012) 137–161.
- [24] S.C. Wei, J. Yang, Forcing through tumor metastasis: the interplay between tissue rigidity and epithelial–mesenchymal transition, *Trends Cell Biol.* 26 (2016) 111–120.
- [25] R. Kalluri, R.A. Weinberg, The basics of epithelial–mesenchymal transition, *J. Clin. Invest.* 119 (2009) 1420–1428.
- [26] J.H. Tsai, J. Yang, Epithelial–mesenchymal plasticity in carcinoma metastasis, *Gene Dev.* 27 (2013) 2192–2206.
- [27] J.H. Tsai, J.L. Donaher, D.A. Murphy, S. Chau, J. Yang, Spatiotemporal regulation of epithelial–mesenchymal transition is essential for squamous cell carcinoma metastasis, *Cancer Cell* 22 (2012) 725–736.
- [28] R.S. Kalra, C.T. Cheung, A. Chaudhary, J. Prakash, S.C. Kaul, R. Wadhwa, CARF (Collaborator of ARF) overexpression in p53-deficient cells promotes carcinogenesis, *Mol. Oncol.* 9 (2015) 1877–1889.
- [29] C.M. Gutschalk, A.K. Yanamandra, N. Linde, A. Meides, S. Depner, M.M. Mueller, GM-CSF enhances tumor invasion by elevated MMP-2, -9, and -26 expression, *Cancer Med.* 2 (2013) 117–129.